Numerical study of a Tesla turbine

N. Huybrechts, O. Berten, E. Lenclud
Free University of Brussels, Applied Mechanics Department
Av F. Roosevelt 50, 1050 Brussel
email: nhuybrec@ulb.ac.be, oberten@ulb.ac.be, elenclud@ulb.ac.be

Abstract: **The turbine, invented by Nikola Tesla (1856-1943), is a bladeless turbine. In this article, we visualize and analyze the flow in this turbine with a commercial CFD software. First, we present the information from the literature that we retain for the construction of the numerical model. Then, we present the numerical model and the used mathematical models. Finally, we analyze the results of the simulation.**

Keywords: **bladeless turbine, computational fluid dynamics (CFD)**

I. Introduction

A. Context of the study

The literature on the bladeless Tesla turbine is very ambiguous. Many different values of the efficiency are available. These values, which are between 2,9%[1] and 106%[2], are generally delivered without computation details. The value above 100% isn't physical and probably comes from computation error. It illustrates the lack of serious of certain studies.

The great disparity of the available information attracted the curiosity of the Applied Mechanics Department, which decided to lead its own study to clarify and supplement this information.

The work is divided in two parts: a bibliographical research and a numerical study.

As the literature doesn't contain enough experimental data, it was necessary to build an experimental model to validate the simulation. The experimental work is realized by M. Wyart [3].

B. Objective of the study

The objective of the bibliographical research is to find the operation principle of this turbine and the characteristics of the geometry. From the literature, we established a list of the parameters, which influence the turbine performance, and a list of the advantages, which are quote there.

The objective of the numerical study is to visualize and analyze the flow in a bladeless turbine with commercial CFD software: Fine. We choose a qualitative approach. Indeed, the influence of the parameters on the flow characteristics is analyzed.

II. Operation principle

The turbine, invented by Nikola Tesla between 1911-1913, is characterized by its bladeless.

A rotor and a carter compose the turbine. The rotor is formed by a set of parallel discs (1), which are assembled on a shaft (2). The discs are spaced (3) to offer a flow section to the fluid injected by a nozzle (4) at the periphery. The fluid trajectory between the discs is a spiral (5). During its trajectory, the fluid drives the discs in a rotational movement. The fluid escapes by the disc holes (6), enters in the exhaust pipe (7).

The turbine allows using different working fluid: air, water, combustion gases, steam.

The space between the discs measures a few millimeters. This value comes from a compromise. With a small space, the nozzle doesn't inject enough fluid to entrain the discs. With a large space, the fluid crosses the turbine without transferring its energy.

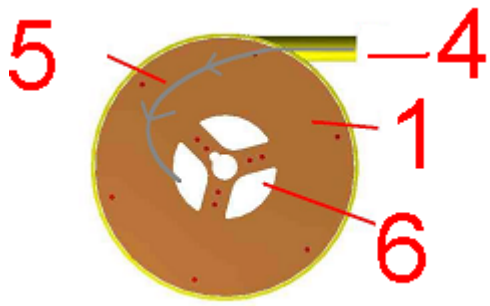

Fig.1.a Operation principle. Profile view

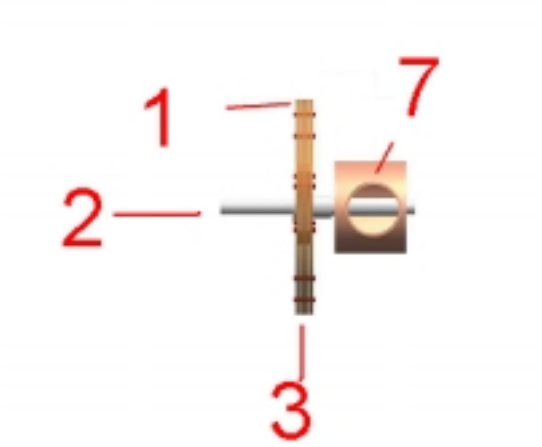

Fig 1.b Operation principle. Side view

III. Bibliographical Synthesis

A. Experimental data

The experimental data on the Tesla turbine are rare, often incomplete or not reliable.

Three prototypes were built at the time of Tesla by " the Allis Chalmers Manufacturing Company". The 457,2 mm (18 inches) prototype rough 150 kW at 10.000 t/m. The maximum efficiency rough 38%. The weak efficiency and some problems with disc distortion brought the end of the collaboration between N. Tesla and the company [4].

In the years fifty, several theses were realized by some American universities [1], [5] and[6]. These works offer the most complete experimental data. The size of the prototype is 152,4 mm and 177,8 mm (6 and 7 inches) and they use air as working fluid. These theses are used to validate the numerical results.

More recently, some studies were achieved by M. Ribaud [7] and M. Singleton [8]. M. Ribaud realized an analytical study of the Turbine Tesla. M. Singleton built a prototype, which follows the design proposed by N. Tesla.

B. Parameters

From the literature, we establish a list of parameters that we analyze the influence on the numerical model. The parameters are the following:

1. The space between the discs: this parameter influences the wall stress and the torque through velocity gradient.
2. The Angle of the nozzle: this parameter changes the length of the streamlines. The objective is to determine if the length of the streamlines influence the energy transfer.
3. The nozzle number: a second nozzle allows increasing the torque. The objective is to determine the influence of the second nozzle on the streamlines and the energy transfer.
4. The boundary layer regime: this parameter influences the energy transfer.
5. The ratio between the inner and the outer radius: this parameter influences the torque value. To analyze this parameter, two prototypes of different size are built. The first prototype has a disc diameter of 254 mm and the second one has a disc diameter of 152 mm.

C. Advantages

From the literature, we also establish a list of quote advantages. These advantages aren't generally validated. Thus, it is necessary to stay critical towards them. The advantages found in the literature are:

1. Better resistance to wet vapor and impurities than conventional turbines [9].
2. Self-regulation: when, from an equilibrium state, the resistive torque increases, the inlet mass flow increases and the streamline length decreases. The decrease of the streamlines length increases the shaft torque and brings the turbine back to the equilibrium state [4].
3. White noise: the loudness spectrum doesn't depend on the angular velocity [9].
4. Weak vibration of the turbine [9].
5. Better resistance to high temperature than conventional turbine [9].
6. Easy to build [9].
7. Reversible: the turbine can be used as pump for liquids or blower for gases.
8. Inversion of the rotational direction: if two nozzles are placed one opposed to the other, the rotational direction is imposed by the selection of the appropriate nozzle.

IV. Numerical Model

To reduce the mesh generation time and the computation time, we only analyze the flow between two co-rotating discs.

To eliminate the generation of an unsteady flow, the bolts (1) aren't modeled and the geometry of the exhaust holes (2) is simplified.

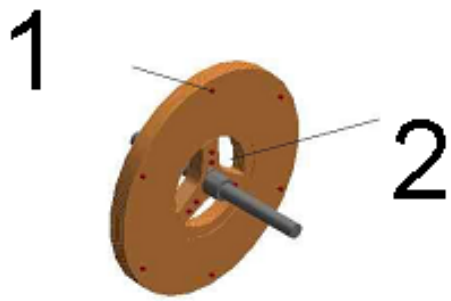

Fig. 2. The experimental rotor

Fig. 3. The numerical rotor

The nozzle tube isn't modeled which means that the boundary conditions are imposed at the disc periphery.

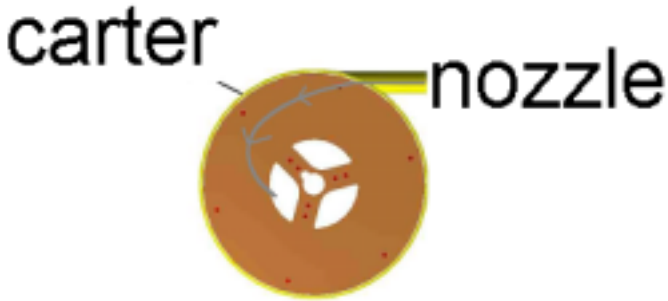

Fig. 4. The experimental nozzle

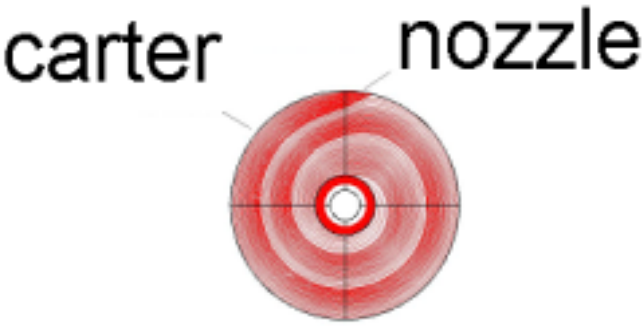

Fig. 5. The numerical nozzle

The length of the exhaust pipe is chosen superior to the establishment length to stabilize the flow before the numerical outlet. While the flow leaves the space between the discs, it must change abruptly its direction. The flow is also influenced by the shaft movement. The flow is thus highly perturbed (see annotation 1 in fig. 7.).

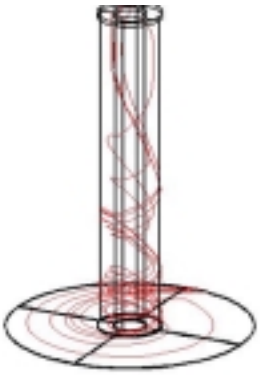

Fig.6. The numerical exhaust pipe

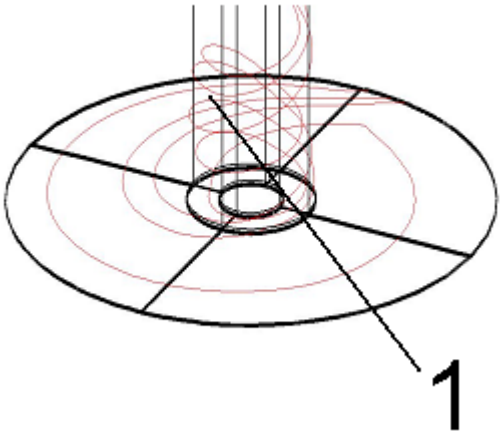

Fig.7. The flow perturbation

The air is chosen as working fluid to compare the simulation with experimental data from the literature.

For the same reason, the dimensions of the numerical models are 125 mm (as [1]) and 254 mm (as [7]).

V. Mathematical Models

The Navier Stokes equations are discretized by a centered Volume finite method. The flow is assumed to be steady, compressible and turbulent. The turbulence model is the Algebraic Baldwin Lomax model. To accelerate the convergence, a multigrid method is used with 3 grid levels.

The mesh is a structured multiblock grid. The mesh size is 134.912 cells for the 254 mm model and 228.384 cells for the 152 mm model. The mesh is refined near the walls to capture the details of the boundary layers and in the transition area. The mesh between the discs is plotted in fig. 8. The grid is refined near the disc (1). For the boundary layer, the grid is also refined near the carter (2). The transition zones are near the nozzle (3), the disc holes (4) and at the inlet of the exhaust pipe.

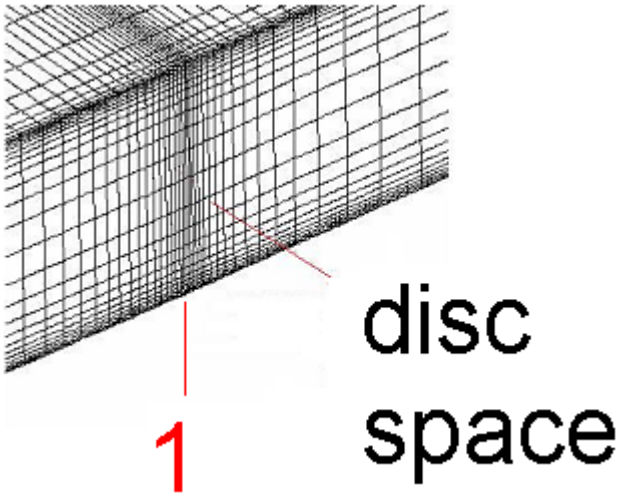

Fig. 8. Mesh in the disc space

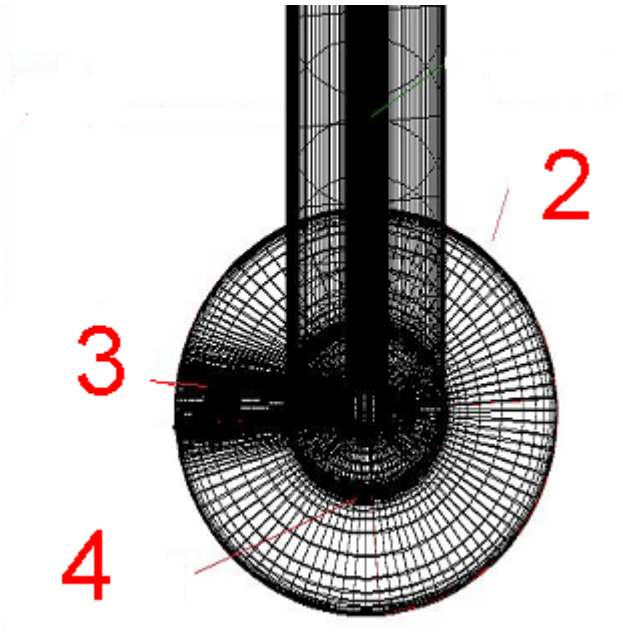

Fig. 9. Grid refinement

VI. Boundary conditions

At the inlet, a flow angle (represented by the normalized radial velocity $\frac{Vr}{V}$), a total temperature and a total pressure are imposed.

At the outlet, the atmospheric pressure is imposed.

On the wall of the shaft and the discs, the angular velocity is imposed.

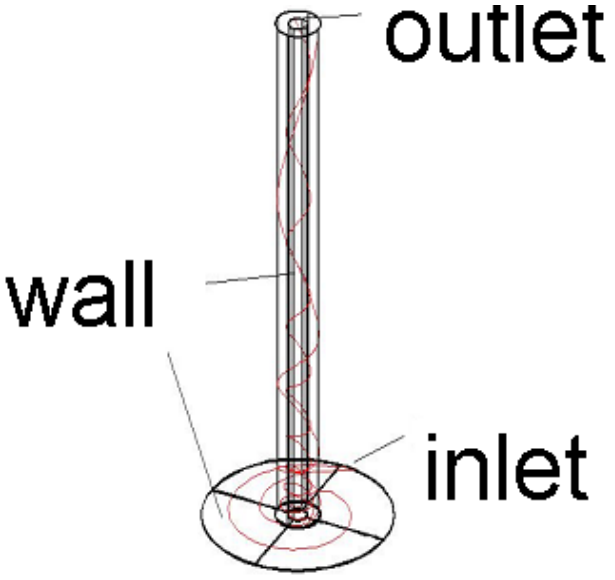

Fig. 10. Location of the boundary conditions

VII. Results

A. Introduction

In this work, we visualize and analyze the flow to understand the way by which the fluid transfers its energy to the discs. From this analysis, three types of losses are detected.

The presence of a boundary layer is discussed. The energetic performances of the turbine are also plotted. The objective is to give some values of the torque, the rotor power and the efficiency.

B. Energetic performance

The angular velocity and the total pressure ratio between the inlet and the outlet of the turbine are chosen as parameters.

For a defined total pressure ratio, the torque, the power and the efficiency are computed for different angular velocities. Then, these values are computed for a defined angular velocity and different total pressure ratio. These curves are plotted for the 152 mm turbine.

In both cases, the nozzle angle is constant too and one nozzle is used.

The torque is obtained from the numerical simulation. The rotor power and the efficiency are defined as:

Definition 1 Rotor power (P_r) and efficiency (η)

$$P_r = C.N$$
$$P = q_m.dH$$
$$\eta = \frac{P_r}{P}$$

C: the torque
P: the reference power
q_m : the inlet mass flow
dH: the total enthalpy difference

1) Constant total pressure ratio

At the inlet, the boundary condition is constant: total pressure (160.000Pa), total temperature (350 K) and normalized radial velocity ($\frac{Vr}{V}=0,86$).

The torque, and the rotor power are plotted below.

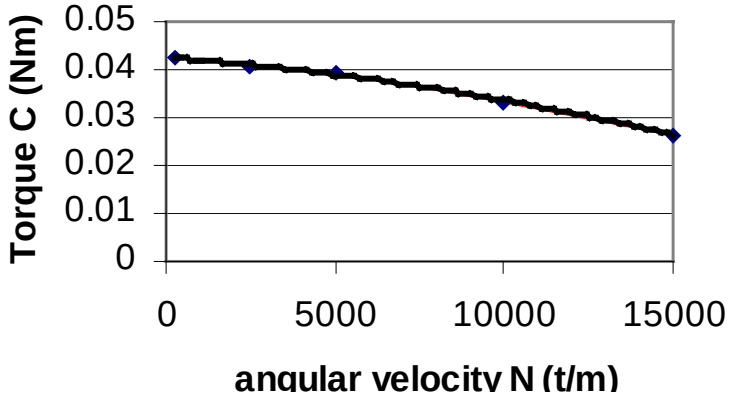

Fig. 11. Torque evolution

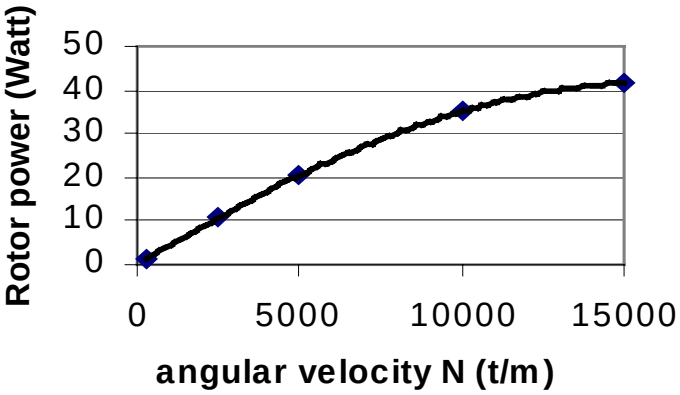

Fig. 12 Power evolution

In fig. 11, it is observed that the torque decreases when the angular velocity is increased. When the angular velocity is increased, the slip between the fluid velocity and the disc velocity. Thus, the viscous effect and the torque decrease. As the torque decreases, the turbine is statically stable.

In fig. 12, it's observed that the rotor power reaches 43,9 W. The efficiency curve follows the rotor power one because the reference power is quasi constant. The efficiency reaches 32%. The rotor power increases because the increase of the velocity is more important that the torque decrease. For high angular velocity, the effect of the torque decrease is the most significant. Thus, the rotor power curve has a maximum value then decreases.

The numerical efficiency is over estimated because the mechanical losses and the air friction losses, the bolt effects, the internal linkages are neglected.

2) Constant angular velocity

The nozzle angle (as above) and the angular velocity (2500 t/m) are constant.

The torque versus the total pressure ratio is plotted in fig.13

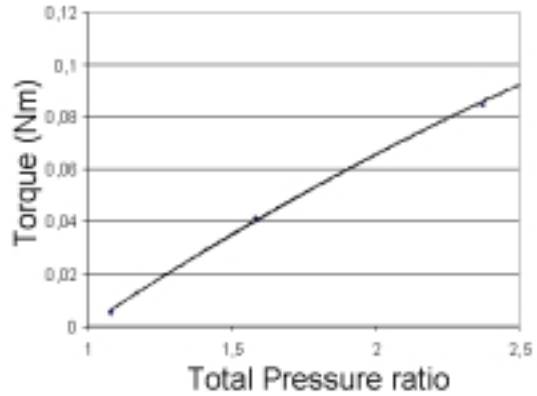

Fig.13. Torque versus the total pressure ratio

In fig13, it is observed that the torque increases when the total pressure ration is increased. As the total pressure is increased, the fluid velocity, the viscous effect and thus the torque increases.

As the reference power is more increased than the rotor power, when the total pressure ratio is increased, the efficiency decreases.

C. Losses

From the flow visualization, the presence of three types of losses are detected: the windage losses, the losses of kinetic energy at the exhaust, losses by friction between fluxes.

1) Windage losses

When the fluid drives the disc in a rotational movement, the stress on the disc wall is positive. This means that the fluid gives its energy to the rotor.

In fig.14, the wall stress on the discs is plotted; it is observed that a negative zone of the wall stress exists near the disc periphery. The black line separates the positive stress (in red) from the negative one (in blue).

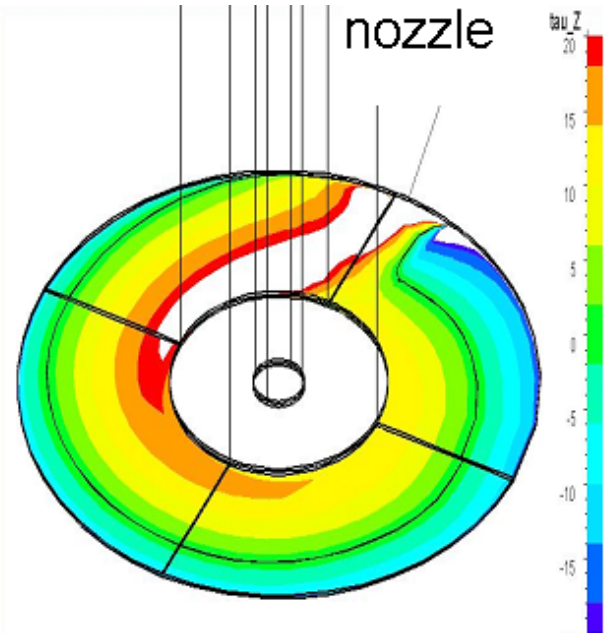

Fig. 14. Windage losses

The presence of negative stress means that the fluid is entrained by the disc. In this zone, the fluid receives energy from the rotor. The turbine is locally used as a blower.

This phenomenon is the windage losses. The windage losses increases when the angular velocity is increased.

2) Losses of kinetic energy at the exhaust

The fluid leaves the space between the discs without transmitting all its kinetic energy. In fig.15, the path line and the velocity distribution are plotted. The fluid velocity in the nozzle is 260 $\frac{m}{s}$. The fluid velocity near the disc holes is 45 $\frac{m}{s}$. This kinetic energy is lost.

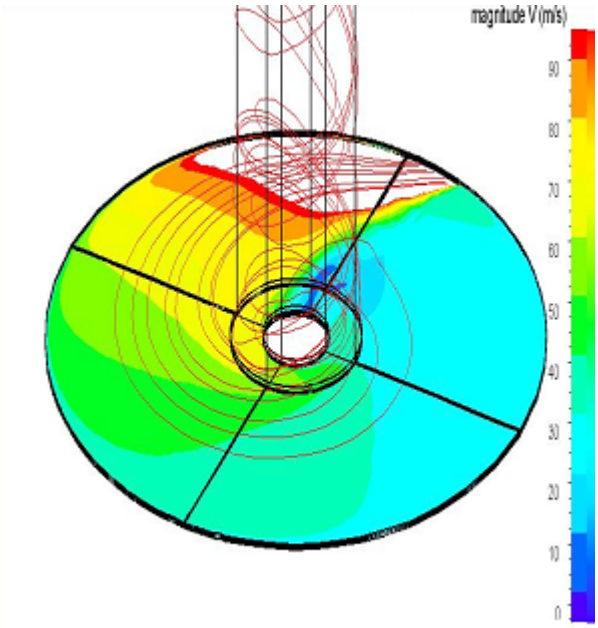

Fig. 15. The exhaust losses

To decrease these losses; the fluid must stay longer between the discs.

The fluid path can be increased with the angular velocity. If the angular velocity is increased, the centrifugal forces compensate longer the radial pressure gradient.

3) Friction losses between fluxes

The high velocity fluid injected by the nozzle is in contact with slower fluid. The slower fluid has already turned once around the disc and has given a part of its kinetic energy. By viscosity effect, the injected fluid drives the slower fluid. A part of the kinetic energy of the injected fluid is thus lost for the rotor.

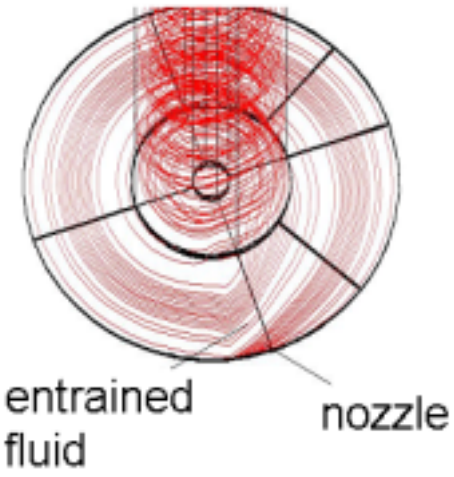

Fig.16. Losses by friction between fluxes.

D. Existence of a boundary layer and flow regime

As boundary condition, a uniform velocity profile is imposed. In fig 17, the velocity profile is plotted just behind the nozzle. On this fig17, the presence of a boundary layer and an external flow are observed.

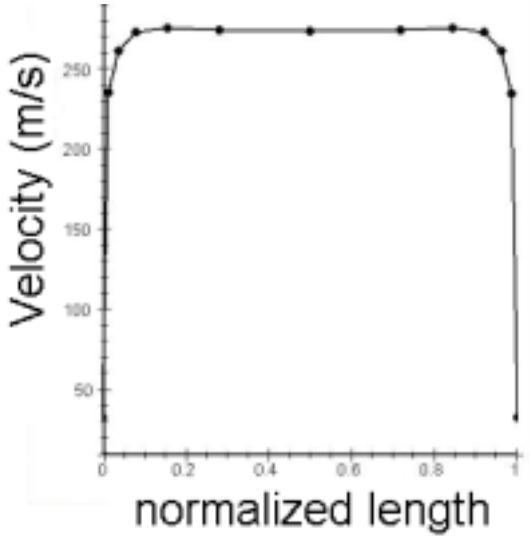

Fig. 17. Profile near the nozzle

When the fluid moves away from the nozzle, the boundary layer grows up and ends to be thicker than the space between the discs (see Fig. 18.). The external flow doesn't exist any more. The flow is purely viscous.

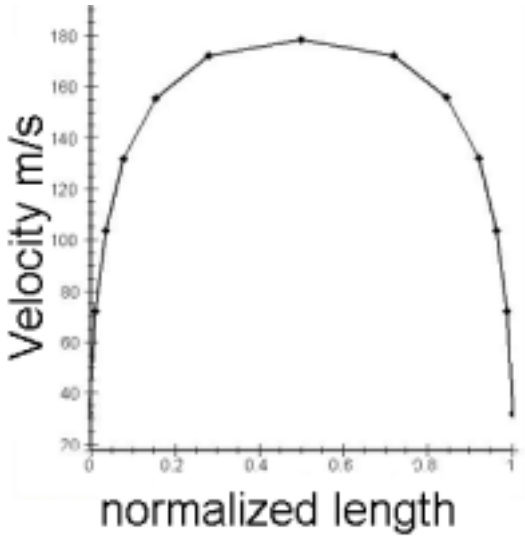

Fig. 18. Profile away from the nozzle.

To know the flow regime, the distribution of the ratio between the turbulent and the viscous viscosity is plotted (Fig. 19.) in a parallel plan with the discs. The plan is located in the external layer. The plotted values are between 0 and 1.

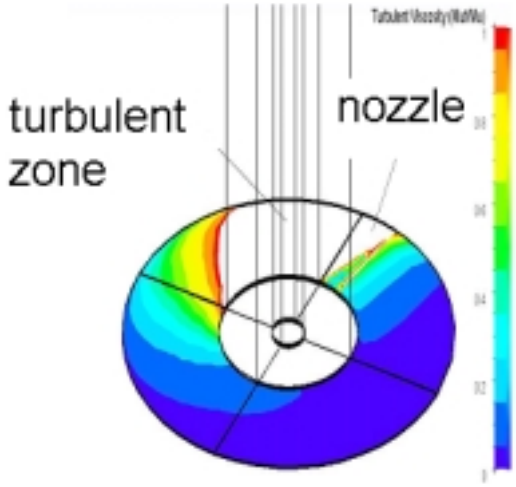

Fig. 19. Flow regime

On this figure, two zones are observed: a turbulent zone where the ratio is superior to 1 and a laminar zone where this ration is inferior to 1. The flow is thus turbulent in the nozzle area and becomes gradually laminar between the discs.

E. Influence of the parameters on the losses

1) The studied parameters

On this section, we analyze the parameter influence on the flow and the losses. The studied parameters are the space between the discs, the nozzle angle, and the number of nozzles.

2) Space between the discs

To analyze the influence of this parameter, several prototypes with different spaces between the discs are built. The spaces between the discs are 0,5 0,8 1 1,2 2 mm. The boundary conditions are kept constant.

In fig.20, the distribution of the stress is plotted on the wall discs for the extreme space (0,5mm and 2mm).

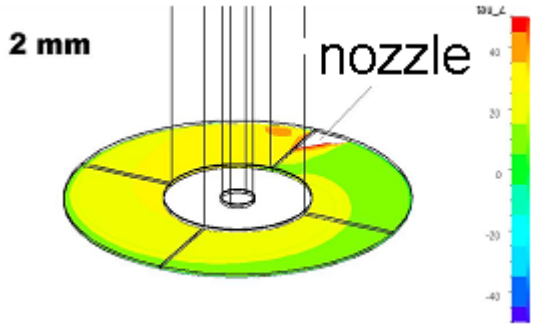

Fig. 20a. Stress distribution for 2 mm

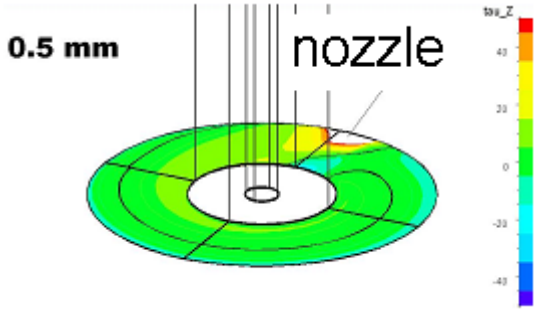

Fig. 20b.Stress distribution for 0,5 mm

In fig 20a (2 mm), the stress distribution is quasi uniform. In fig 20b (0,5 mm), an extended zone of negative stress is observed.

On average, the stress has a higher value for the 2 mm space than with the 0,5 mm space. Thus the torque is more important.

With the 2 mm space, the exhaust losses are important. The fluid fell less the presence of the discs and only transfer a part of its kinetic energy.

With the 0,5 mm space, the windage losses are preponderant. The exhaust losses are weak because the fluid fell strongly the disc presence.

The optimum for the space between the discs comes from a compromise between the losses and is equal to 1 mm.

3) Nozzle angle

In this section, the influence of the nozzle angle on the energy transfer is studied.

For a quasi-radial nozzle, the path lines are plotted in fig 21. On this figure, it is observed the fluid goes directly to the exhaust pipe.

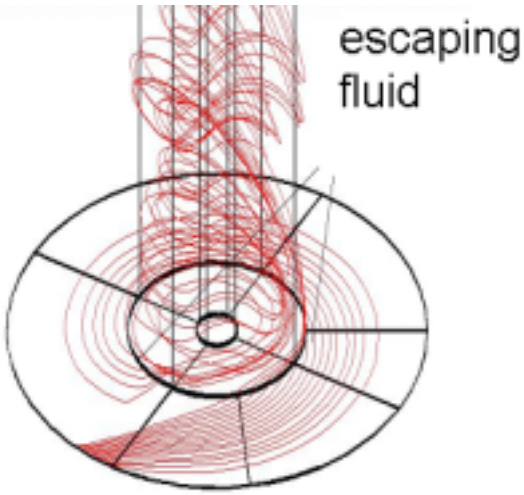

Fig.21. Path lines for a quasi-radial nozzle

When the normalized radial velocity is increased, the exhaust losses increase. The losses by friction between fluxes decrease because the entrained mass flow decreases. The

optimal normalized radial velocity comes from a compromise between the losses and its value is between 0,6 and 0,7.

4) Number of nozzles

In this section, the influence of a second nozzle on the flow characteristics is analyzed. The second nozzle is placed on the other side of the discs for the prototype of 152 mm.

In fig.22 and 23, the distribution of the wall stress is plotted for the configuration with one and two nozzles.

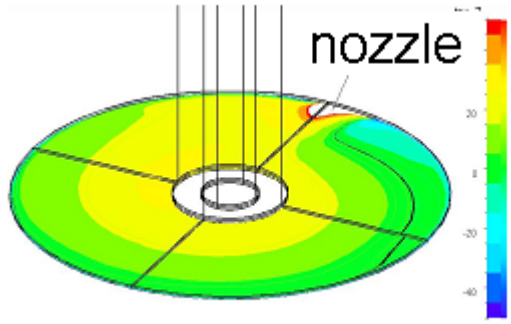

Fig. 22.Stress distribution for one nozzle

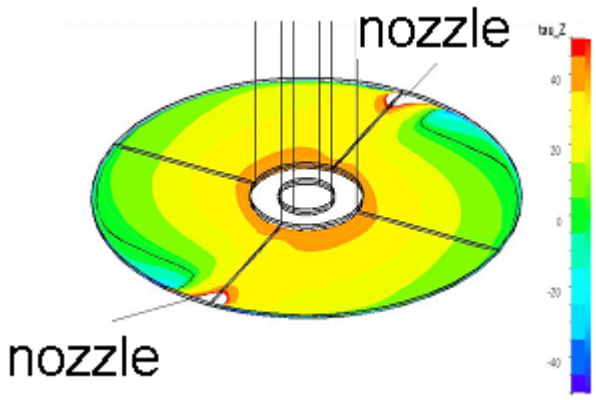

Fig. 23. Stress distribution for two nozzles

On average, the stress level and the torque are superior with the second nozzle. The windage losses are more localized but the presence of the second nozzle drive the fluid from the other nozzle out the space between the discs. The exhaust losses increase. The second nozzle is thus interesting when the windage losses are preponderant in the one nozzle configuration and must be misadvised when the exhaust losses are already preponderant.

VIII. Conclusions

From the literature, we establish a list of parameters, which influence the flow ad the energy transfer. These parameter influence are analyzed on the numerical model. From the flow visualization and analyze, three types of losses are found: the windage losses, the exhaust losses and the losses by friction between fluxes.

To increase the performance of the bladeless turbine, a compromise between those losses must be done.

The parameters influence the losses. For each parameter, an optimal value is found.

To reduce the exhaust losses, which are the most crucial, the angular velocity must be increased and the space between the discs must be decreased.

To increase the turbine power, the number of nozzles and discs must be increased.

IX. Perspectives

In a future study, it will be interesting to analyze the influence of the disc number and to use more viscous fluid.

The influence of the disc holes and the exhaust pipe must be also analyzed.

Acknowledgements

I would like to thank Pr B. Leduc to have proposed this subject of work and to have accommodated me in its service. I would also like to thank Mr O. Berten and E. Lenclud to have supervised this work.

References

[1] Robert K. Warner, *The design, construction and testing of a Tesla turbine*, MS thesis, University of Maryland, 1949

[2] Viscotherm, http: //www.geocities.com/viscotherm/tesla.htlm

[3] E. Wyart, *Etude préliminaire d'une turbine Tesla: Aspect experimental*, Travail de fin d'études, ULB, 2002

[4] Tesla Engine Buiders Association, *Membership manual*, 1999

[5] W. Rice, *An analytical and experimental investigation of multiple disk-turbines*, Journal of engineering of power, trans. ASME, july 1965, pp23-36

[6] Y. Ribaud, E Laroche, *An analysis of the internal aerodynamics losses produced in the lamina and centrifugal flow between rotating discs*, 3rd European conference on turbomachinery-fluid dynamics and thermodynamics, London, March 1999

[7] C. Singleton, *The investigation and analysis of Nikola Tesla 's bladeless turbine*, Queensland University of Technology, 2000

[8] Audley B. Leaman, *The design, construction and investigation of a Tesla turbine*, MS thesis, University of Maryland, 1950

[9] R. Jacobson, *The Tesla bladeless pumps and turbines*